



Experimental Assessment of Plate Heat Exchanger Performance Enhancement by Compound Pulsating and Low Concentration CuO Nanoadditive Methods

Amina H.D. Alikhan^{*}, Khaleel S.J. Al-Ogaili, Hadi O. Mery

Mechanical Department, College of Engineering, Wasit University, Kut 52001, Iraq

Corresponding Author Email: adhaef@uowasit.edu.iq

Copyright: ©2025 The authors. This article is published by IETA and is licensed under the CC BY 4.0 license (<http://creativecommons.org/licenses/by/4.0/>).

<https://doi.org/10.18280/ijht.430205>

ABSTRACT

Received: 22 January 2025

Revised: 11 March 2025

Accepted: 26 March 2025

Available online: 30 April 2025

Keywords:

Brownian motion, CuO-water nanofluids, performance evaluation criteria (PEC), plate heat exchanger, pulsating flow

High nanoparticle concentrations in a base fluid may cause problems such as sedimentation, increased pumping power, and costs. Many experimental and numerical studies show the possibility of improving heat transfer in various engineering applications using small nanoparticle concentrations. The objective of the present study is to assess the thermal performance enhancement by compound pulsed flow and low-concentration CuO-water nanofluid in compacted plate heat exchangers. The assessment has been performed through experimental measurements with the pulsed flow at frequencies of 3 Hz, 5 Hz, and 10 Hz of CuO nanoparticle concentrations of 0.01%, 0.05%, 0.1%, 0.2%, 0.4%, and 0.6% by weight. The friction factor, Nusselt number, and their combinations were used as criteria to evaluate and compare the performance of the compacted heat exchanger. The experiments revealed that the Nusselt number, heat transfer rate, and efficiency of the tested heat exchanger were significantly enhanced when the pulse frequency was increased from 3 Hz to 10 Hz. The Nusselt number improved by 36% at the maximum frequency of 10 Hz and CuO concentration of 0.6 wt.%. The heat transfer rate also improved with increasing pulse frequencies and concentrations from 0.01 wt.% to 0.6 wt.%, where the heat transfer rate increased by 2%-12% at 3 Hz, 7%-25.5% at 5 Hz, and 14%-36% at 10 Hz. Finally, the highest performance evaluation criteria (PEC) were obtained at 0.2 wt.% CuO concentration, and 10 Hz pulse frequency. A further increase in the nanoparticle concentration above 0.2 wt.% was proved to be ineffective.

1. INTRODUCTION

The approach of utilizing nanofluids to improve heat transfer in a variety of engineering applications has been widely investigated. Early in 1995, Choi and Eastman [1] demonstrated that the heat transfer capacity was increased by adding solid particles, including metal oxides, with sizes much smaller than 100 nanometers to the base fluid. The subject of nano-enhanced heat transfer in engineering equipment has been widely studied and reviewed, e.g., by nano-in base fluid [2-5]. Al-Kayiem et al. [6] reviewed the thermal enhancement by nanomaterials for thermal energy storage technologies, and Sarkar [7] reported a review on convective heat transfer correlations of nanofluids.

The applications of heat exchangers have advanced significantly in engineering due to their inherent privileges, obtained through the execution of passive, active, or combined improvement techniques. Al-Kayiem et al. [8] reported that the heat transfer enhancement is either (i) active methods, which use an external power source, or (ii) passive methods, which use several techniques without a power source such as turbulence generators (as a propeller, spiral fin, twisted tapes, ribs, ..., etc.) or by improving the thermal fluid properties using additives like the nanoadditives. However, they also named a third enhancement technique (iii) compound heat

transfer enhancement, when two passive or active methods are used simultaneously. In addition, Al-Kayiem [9] introduced, through his implementation of a special issue as guest editor, a wide scope on the reliability of nanoadditives on the thermal enhancement of nanofluids and their applications.

Particularly, enhancing heat transfer in various heat exchanger applications using nanofluids instead of the base fluid has been introduced by many investigators. Zhang et al. [10] compiled the research on nano-enhanced heat exchangers and reported a critical review of the nanoadditives effect on enhancing the performance of plate heat exchangers (PHEs). They emphasized that PHEs provide a large contact area by diffusing hot and cold fluids on the plates, in addition to their other advantages of low pollution and maintenance. According to Singh et al. [11] and Shamshirgaran et al. [12], the introduction of nanoparticles into working fluids has revolutionized heat transfer efficiency by enhancing thermal conductivity and overall system performance. Sequel to Saranya et al. [13] and Wang et al. [14], emphasized that advancement enables the development of more compact, energy-efficient systems, making them essential for various industrial applications such as cooling systems, power generation, and chemical processing.

Naphon and Wiriyaart [15] presented an experimental study for heat transfer enhancement under the influence of the

pulse frequency of nanofluids in the presence of a magnetically influenced micro fin tube. The study shows it is possible to improve heat transfer by increasing the concentration of nanoparticles and introducing magnetic fields. Other studies, like Muley et al. [16], Khan et al. [17], and Kumar et al. [18], have investigated optimizing heat transfer by regulating and controlling various operational and design parameters of PHEs, including flow rate, temperature, chevron angle, and nanoparticle loading. In another compound enhancement technique, Al-Kayiem et al. [8] explored the influence of compound 0.1 vol.% TiO₂-in-water nanofluid with multiple twisted tape inserts on the hydrodynamic performance of double pipe heat exchangers. Results showed a maximum increase of 110.8% in Nusselt number in a tube fitted with quintuple twisted tape inserts, with a 25.2% increase in the pressure drop.

For instance, Akhavan-Behabadi et al. [19] studied the influence of both geometric modification and MWCNTs on the heat transfer rate, observing at certain nanoparticle concentrations, an 85% increase in the heat transfer rate and a 475% increase in the pressure drop at high Reynolds numbers. Similarly, Xie et al. [20] and Jamshidi et al. [21] determined the optimal nanoparticle concentrations in a range of 0.5%-2% to enhance the thermal performance in the convective systems and helical tubes, respectively. Corcione et al. [22-24] performed numerical studies to determine the optimum nanoparticle concentration to maximize the heat transfer under both laminar and turbulent flow regimes, ensuring the maintenance of the heat transfer rate while minimizing the operational costs. Further research by Mukeshkumara et al. [25] and Kumar et al. [26] explored the relationship between the pressure drop, heat transfer coefficient, and the concentration of Al₂O₃ in shell and helically coiled tube heat exchanger, and it was found that the Nu increased with increasing of volume concentration from 0.4% to 0.8%. The results showed that increasing the volume concentrations of nanoparticles from 0.1%, 0.4%, and 0.8% increased Nu by 21%, 28%, and 42%, and increased the pressure drop by 8%, 12%, and 20%, respectively.

However, high nanoparticle concentration often led to an increase in the pressure drop and deterioration of the performance of heat exchangers. This fact is experimentally approved by Shamshirgaran et al. [27] in their investigation of thermal performance, pressure drop, and pumping power in a Cu-water nanofluid-filled flat plate solar collector. Also, Choi et al. [28] investigated that adding a small volume concentration of nanoparticles to the base fluid caused a significant increment in the thermal conductivity of the base fluid. In comparison, Diao et al. [29] observed that adding nanofluid to multiport mini channels increased both pressure drop and friction factor, with optimum performance at lower concentrations. In a parallel approach, Oliveira et al. [30] found that the increase in MWCNT concentration leads to increased viscosity as well as thermal conductivity. Further, Huang et al. [31] confirmed that an increase in MWCNT concentration also leads to increased viscosity but decreases the heat transfer due to raising the pressure drop and friction coefficient in a plate heat exchanger. Sharafriz and Hormozi [32] investigated adding MWCNT to base fluid enhanced thermal conductivity by about 68%, accompanied by elevating the friction coefficient in the PHE.

Previous studies have highlighted the need for an alternative solution to optimize the heat performance of nanofluids while minimizing the associated pressure drop. To that end, the use

of high-concentration nanoparticles is avoided, while low concentration ones are utilities. One effective technique involves improving the fluid mixing and generating a vortex, which can be obtained by tailoring the flow pattern and increasing the turbulence at the inlet. For instance, Naphon and Wiriyasart [15] and Wang and Zhang [33] utilized a range of pulsating flows to enhance the Brownian motion and turbulences. At the same time, Alikhan and Maghrebi [34] and Alasady and Maghrebi [35] experienced the impact of constant pulsating flow on the plate heat exchanger performance with hybrid nanofluids. The results demonstrated that applying the pulse frequency with low hybrid nanoparticle concentration enhanced the Nu and slightly increased pressure drop.

On the other hand, Najafabadi et al. [36] showed that increasing the size of the nanoparticle contributes to improving the Nu but increases the friction coefficient. Meanwhile, Surendar et al. [37] focused on improving the thermophysical properties by adding the makeup metals and carbides of nanoparticles to the base fluid. The results declared that this method enhances the heat transfer rate of the heat exchanger.

The above studies have demonstrated the challenge of balancing heat transfer improvements with the problem associated with increased pressure drop at high nanoparticle concentrations. Therefore, there is an increasing focus on improving the thermal performance of low-concentration nanoparticles. This study aims to provide an experimental investigation to enhance the HEX performance of compact plates by enhancing the Brownian motion of copper oxide and increasing turbulence via the pulsating flow effect while maintaining the pressure drop within an acceptable limit. To achieve this balance goal, the present study adopts a unified evaluation criteria that includes both heat transfer optimization and pressure drop parameters to evaluate and improve the thermal performance of Chevron plate heat exchangers in general and to know the effect of high concentrations on this balance and to determine the optimum concentration under the operating conditions of this study where the use of high nanoparticle concentrations may be infeasible. The goal is to enhance the heat transfer efficiency while minimizing the negative effects of high nanoparticle concentrations.

2. EXPERIMENTAL METHODOLOGY

The outline of the experimental method involves the investigation of the impact of CuO-water nanofluid at various concentrations under different pulsating flows on the performance of plate heat exchangers. Water-based copper oxide nanofluids with different concentrations ranging from 0.01 wt.% to 0.6 wt.% were provided by Vera Carbo Nano (VCN) Materials Co., Ltd. The mean diameter of additives is 20-30 nm. The purity of additives is +95%. A French-made Zeta Compact Model was used to verify the stability of nanomaterials, as presented in Figure 1. The zeta potential approach yields good accuracy for stability. The experimental work includes setting up the experiments' apparatus, conducting tests under specified conditions, collecting data, and analyzing the results obtained. This experimental procedure might help actually understand the effect of nanofluids and pulsating flow on heat transfer rate and friction factor. The schematic of the experimental setup is illustrated in Figure 2, outlining the whole stages of the experiments.

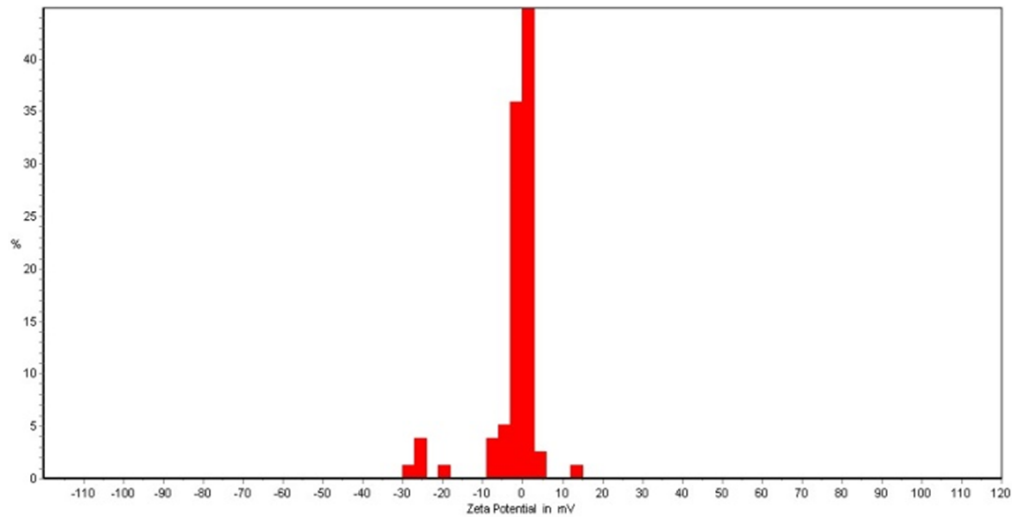


Figure 1. Zeta potential test

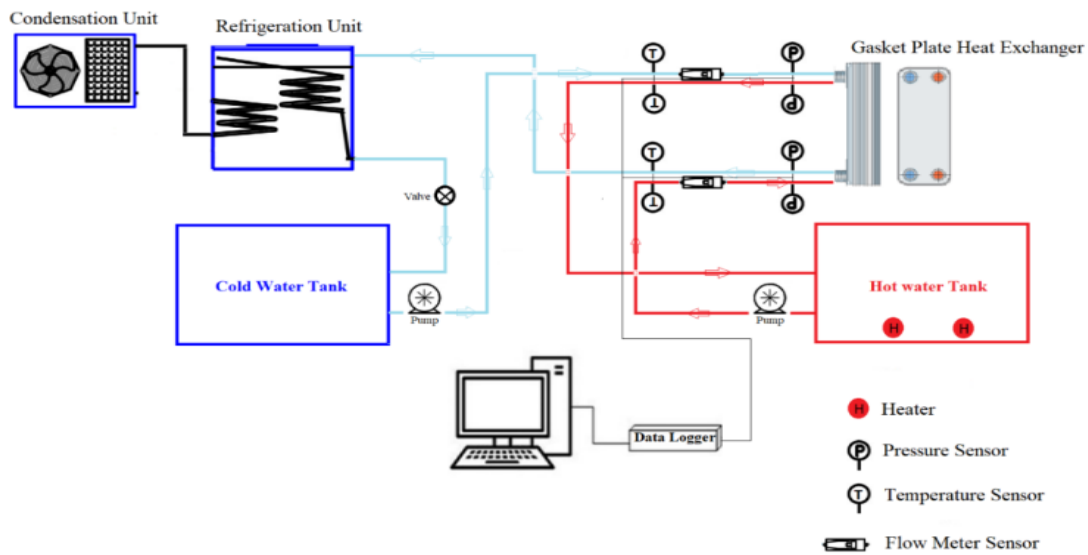


Figure 2. Experimental setup

2.1 Experimental setup

The experimental apparatus mainly consists of an M3 type manufactured by Sana Mobadel Toes Pars Company, a reciprocating pump system, hot and cold fluid loops, and a 10-channel Data Logger made by Toes Nano Company. The continuous nanofluid flow through the PHE in the closed system is done by a 0.65 kW NAVID MOTOR. At the same time, the pulsating flow of nanofluids is performed by the reciprocating pump, which includes a Crank and movable shaft, piston pump, and LS IC5 0.75 kW inverter, which controls the number of pulses per second. The inlet nanofluids temperature must be constant for all tests; therefore, before entering the PHE. The nanofluids are entered into the cooling units, which contain temperature sensors with an error rate not exceeding 0.1%, connected to the data logger, directly displaying three readings per second on the personal laptop. When the temperature reaches the required input temperature, the valve installed on the cooling unit is opened to allow the fluids to pass into the heat exchanger.

The hot water loop comprises a hot water tank of 40 L capacity with two 6 kW immersion heaters. 15 LPM hot water flow rate has a constant inlet temperature at 70°C, while 15 LPM cold fluids enter the test section at a temperature of 40°C.

The pressure, temperature, and mass flow rate are taken by sensors that transmit the values in the form of an Excel file via the data logger. Due to high thermal conductivity, chemical, and physical stability, CuO-water nanofluids with purity equal to 95% are used for this work. The heat exchanger and plate geometrical details are shown in Table 1 and Figure 3.

Table 1. Features of the heat exchanger

Components	Symbol	Value	Unit
Heat exchanger area	A	0.352	m ²
Mean channel spacing	b	2.8	mm
Port diameter	D _{port}	31	mm
Total number of plates	N _t	21	-
Plate width inside the gasket	L _w	91	mm
Vertical distance between centers of ports	L _v	357	mm
Horizontal distance between centers of ports	L _h	60	mm
Plate thickness	t _{plate}	0.5	mm
Corrugation depth	L _{Corr.}	2.7	mm
Hydraulic diameter	D _e	0.44	mm
Gasket thickness	t _{gasket}	0.37	mm
Chevron angle	β	60	-

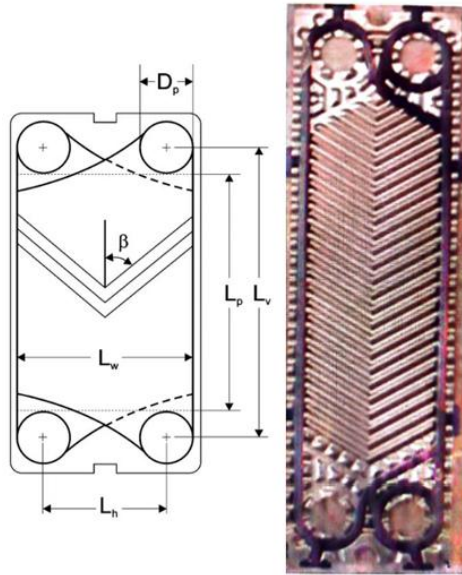


Figure 3. Basic geometric parameters of chevron plate [38]

2.2 Measuring instruments

The following instruments are used:

- Pressure sensors: There are four pressure sensors installed at the inlet and outlet of both the hot and cold sides of plate heat exchangers to capture the pressure value and calculate the pressure drop.
- Temperature sensors: Four temperature sensors are located at the inlet and outlet to sense and calculate the temperature change on both PHE sides.
- Flow meter: Two flow meters are positioned at the inlet of both PHE sides to calculate the flow rate.
- Data logger: This device is used to capture and collect the signals from the experiment sensors and timely record and store them in an Excel file.

The thermophysical characteristics of the used materials are listed in Table 2.

Table 2. Thermophysical characteristics of CuO and water at T=25°C

Materials	Density (kg/m ³)	Specific Heat (J/kg·K)	Thermal Conductivity (W/m·K)	Dynamic Viscosity (kg/m.s)
H ₂ O	997.2	4179	0.613	0.000891
CuO	6320	531.8	76.5	-

2.3 Experimental procedure

The measuring procedure included the following steps:

- (1) Prepare the desired concentration of nanofluids for certain experiments.
- (2) Check and secure all connections, including pipes, sensors, joints, and the plate heat exchanger, ensuring there are no leaks, loose fittings, or improper alignments before starting the experiment.
- (3) Start the pumps of hot and cold fluid to achieve a certain flow rate and temperature.
- (4) Start the reciprocating pump and adjust the frequency by an inverter to generate a certain pulsating flow.
- (5) Monitor the performance and collect data on pressure, temperature, and flow rate at predetermined intervals every 10 minutes throughout the experiment, ensuring

consistent recording on the PC.

- (6) Repeat steps 4 and 5 to apply the new frequency at the same nanoparticle concentrations.
- (7) Repeat the entire procedure with new concentrations of nanoparticle, adjusting the pulsating flow frequencies accordingly while maintaining consistent flow rates and temperatures from previous experiments.

2.4 Uncertainty analysis

The accuracy and precision of measurements are analyzed and assessed to verify the experimental uncertainty. The deterioration in the instrument's performance may result from device limitations, data logger intervals, experimental malfunction, and the impact of environments. The uncertainty of each parameter is calculated and accumulated along with its driven results from sensor records to the final parameter. For instance, the uncertainty of the Nu and friction factor is derived from the temperature and pressure records, taking into consideration the amplification of the error factor while applying the parameter formula. The uncertainties and measurement accuracies of the sensors are presented in Table 3.

Table 3. Sensors accuracy

Sensor	Accuracy	Uncertainty
Temperature	0.1°C	±0.1
Pressure	0.01 mbar	±0.01
flowrate	0.01 L/sec	±0.01

Eq. (1), recommended by Alasady and Maghrebi [35], was also adopted to check the uncertainty, where R represents a function of independent linear parameters. R = (v₁, v₂, v₃, ..., v_n):

$$\delta R = \sqrt{\left(\frac{\partial R}{\partial v_1} \delta v_1\right)^2 + \left(\frac{\partial R}{\partial v_2} \delta v_2\right)^2 + \left(\frac{\partial R}{\partial v_3} \delta v_3\right)^2 + \dots + \left(\frac{\partial R}{\partial v_n} \delta v_n\right)^2} \quad (1)$$

2.5 Estimation of nanofluids properties

The proposed equations by Sarkar [7] are used to compute the nanofluids thermophysical properties as follows:

$$\rho_{nf} = \phi \rho_p + (1 - \phi) \rho_w \quad (2)$$

$$(\rho C_p)_{nf} = \phi (\rho C_p)_p + (1 - \phi) (\rho C_p)_w \quad (3)$$

$$\mu_{nf} = (1 + 2.5\phi + 6.5\phi^2) \mu_w \quad (4)$$

$$k_{nf} = \left[\frac{k_p + 2k_w - 2\phi(k_w - k_p)}{k_p + 2k_w + \phi(k_w - k_p)} \right] k_w \quad (5)$$

3. DATA REDUCTIONS

The set of equations suggested by Corcione et al. [24] and Mukeshkumara et al. [25] have been adopted to determine the thermal properties of the PHE.

$$T_{c,avg} = \frac{T_{c,o} + T_{c,i}}{2} \quad (6)$$

$$T_{h,avg} = \frac{T_{h,o} + T_{h,i}}{2} \quad (7)$$

$$Q = \dot{m} C_p (T_{in} - T_o) \quad (8)$$

$$Q_{avg} = \frac{Q_h + Q_c}{2} \quad (9)$$

$$u = 0.348 Re^{0.663} Pr^{0.33} \quad (10)$$

$$f = \frac{\Delta p}{\left(\frac{L_v}{D_e}\right) \times \left(\frac{2G^2}{\rho}\right)} \quad (11)$$

$$\varepsilon = \frac{Q_{avg}}{C_{min}(T_{h,i} - T_{c,i})} \quad (12)$$

where, C_{min} is the minimum $\dot{m}C_p$.

4. RESULTS AND DISCUSSIONS

To find out the effect of CuO-Water nanofluids used for conducting the experiments at different nanoparticle concentrations under the influence of the pulsed flow at frequencies not exceeding 10 Hz on the heat exchanger performance of Figure 4 and Figure 5 were drawn, which represent the relation between the Nu and the average rate of heat transfer at different concentrations of nanoparticles and for the three frequencies used to conduct the experiments. It is noted that the zero point for each line represents its value for the water at the continuous flow, which is the comparison point for the readings. Figure 4 demonstrates that at the continuous flow, the Nu increases between 7%-26% when the concentration of nanoparticles is increased from 0.01 wt.% to 0.6 wt.%. This occurs due to the increase in thermal conductivity, which exceeds the increase in viscosity when increasing the nanoparticle concentration compared to the base fluid. The same behavior is echoed for other cases, which represent the Nu values at frequencies of 3 Hz, 5 Hz, and 10 Hz, with the difference in the Nu values due to the increase in pulse frequency. The results improve with the increase in turbulence in the boundary layer region, which results from the increase in frequency due to centrifugal force under the influence of the pulsed flow. The pulse flow caused an irregular pressure distribution, which led to an increase in the random motion in the longitudinal and radial directions of the nanoparticles in the base fluid. The increase in the pulse flow frequency from 3 Hz to 10 Hz causes an increase in the Nu due to an increase in the random motion of nanoparticles, where the highest Nu value was obtained at the highest concentration and highest frequency, which was 36%.

Figure 5 presents the variation of heat transfer rate in comparison with various CuO-Water concentrations as well as at various imposed pulsating frequencies. The Brownian motion of suspended nanoparticles in the base fluid is significantly impacted by the frequency pulsing flow. Therefore, the nanofluids with higher pulsating frequency have higher heat transfer rates. The effect of the nanoparticle concentrations and the frequency is noticeable at concentrations higher than 0.1 wt.%. The increase of frequency to 3 Hz causes an increase in the heat transfer rate of about 2%-12%, while it is 7%-25.5% at 5 Hz, and 14%-36%

at 10 Hz when the concentrations increased from 0.01 wt.% to 0.6 wt.%. Comparing the improvement in the average heat transfer and Nu, it is found that 0.2 wt.% with a frequency of 10 Hz achieves the best choice for the studied cases. Compared with the continuous flow, this surpasses the improvement in heat transfer resulting from the highest concentration of nanoparticle used at 0.6 wt.%, which saves on the cost of using high-concentration nanoparticles.

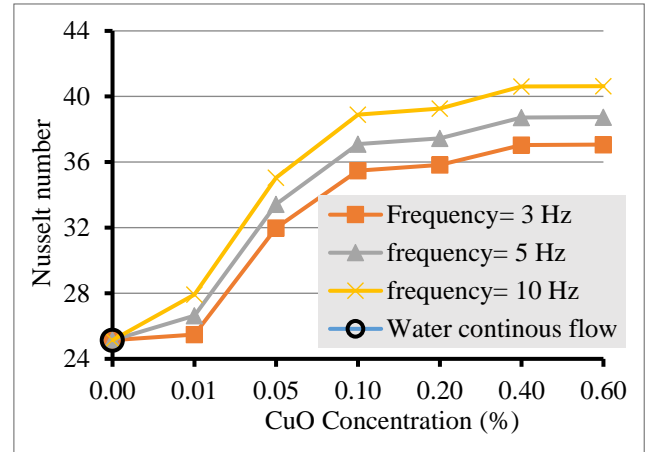


Figure 4. Variation of Nusselt number at different concentrations and frequencies

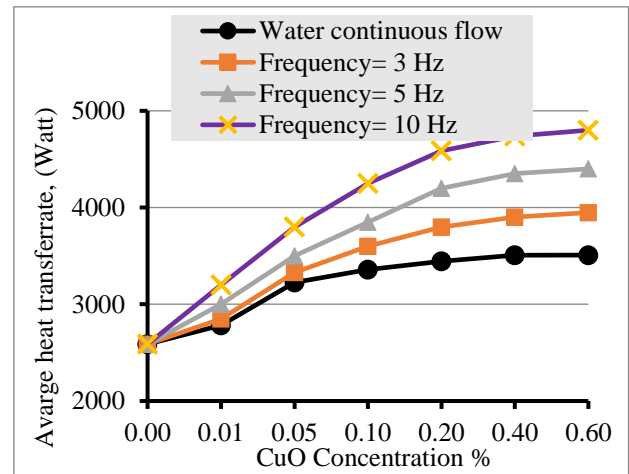


Figure 5. Variation of average heat transfer rate at different concentrations and frequencies

Figure 6 represents the efficiency improvement in the thermal effectiveness of the PHE at 3 Hz, 5 Hz, and 10 Hz with different concentrations of CuO-water nanofluid relative to the water at steady-state laminar flow (also called relative effectiveness (ε_r)). Furthermore, the figure demonstrates the compound effect of the pulsating flow and the addition of particles of copper oxide to the base fluid on the studied heat transfer coefficients and the Brownian motion of these particles. The results of the analysis are provided where the effect of different frequencies and different concentrations are studied. The relative effectiveness is directly related to concentration as well as frequency. This is expected since the increase in secondary mixing resulting from the increase in Brownian motion of nanoparticles under the influence of pulsed flow as the flow enters the dead zone areas and thus increases the heat transfer between the hot and cold liquid to achieve the highest thermal performance for the highest

nanoparticle concentration by 56%.

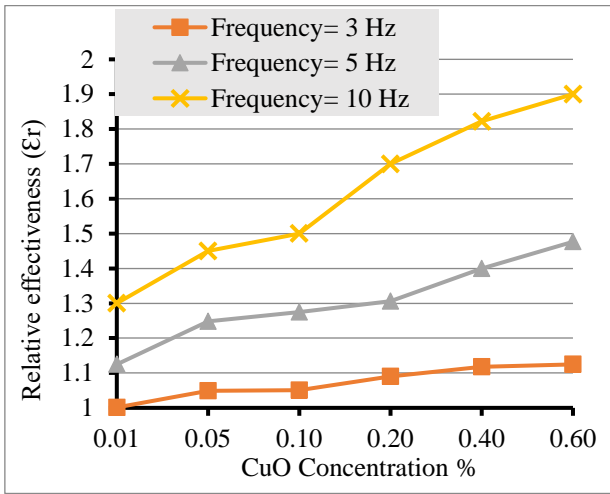


Figure 6. Relative effectiveness at different concentrations and frequencies

Figure 7 represents the change in the friction factor with different concentrations of nanoparticles under the conditions of pulsating flow. It can be demonstrated that the lowest value of the friction factor is for water at continuous flow, where the pulsating flow results in a change in the flow pattern, which in turn leads to an increase in the friction factor. However, it is noteworthy that the increase in the friction factor resulting from increasing the frequency to 10 Hz is relatively small and is less than the increase caused by increasing the concentration from 0.01 wt.% to 0.6 wt.%.

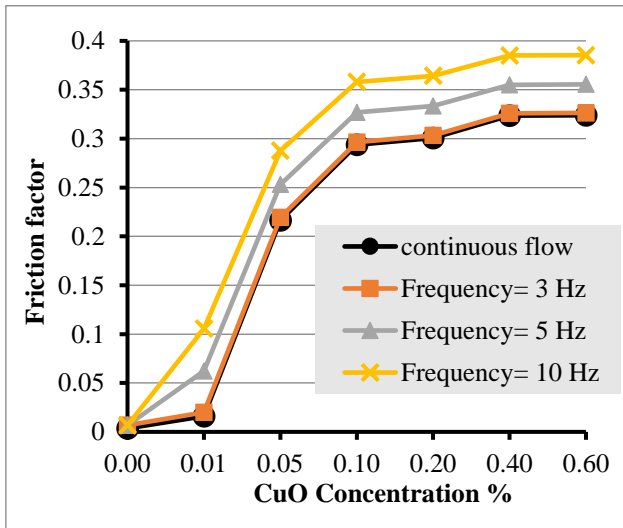


Figure 7. Variation of friction factor at different concentrations and frequencies

Therefore, Figure 8 was developed to show the best thermal performance of the PHE under these conditions, which achieves an increase in the rate of heat transfer and a relatively lower friction factor by prediction of the performance evaluation criterion (PEC), or named performance indicator [39].

$$PEC = \frac{Nu_r/Nu_o}{(f_r/f_o)^{1/3}} \quad (13)$$

where, Nu represents the Nusselt number, and f is the friction

factor, subscription "r" refers to the pulsated and nanofluid case, while "o" refers to the case without pulsation and pure water fluid flow.

Whenever the PEC value is more than one, the thermal performance improvement exceeds the friction value. Otherwise, friction dominates. The highest frequency values reached in the research at different concentrations are presented in Figure 8. The value of PEC increases with increasing concentration, reaching the highest value of 2.2 at a concentration of 0.2 wt.%. However, when the nanoparticle concentration increased higher than 0.2 wt.%, the value of PEC, which is a function of both the Nu and the friction factor, decreases due to the noticeable increase in the friction factor compared to the increase in the Nu.

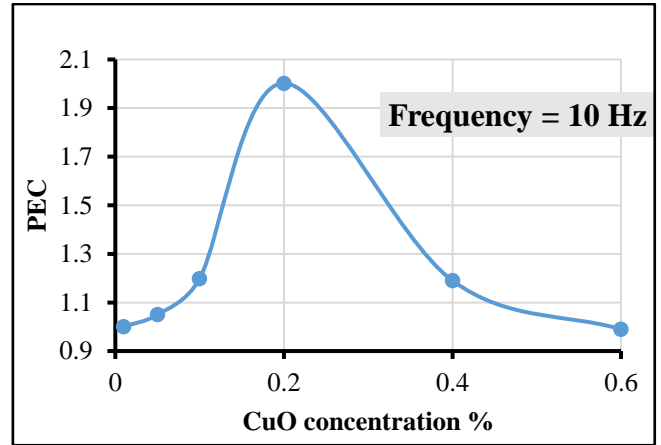


Figure 8. Variation of PEC with different nanoparticle concentrations at a constant frequency

Eqs. (12) and (13) represent a developed correlation of Nu and friction factor in terms of the studied parameters, CuO nanoparticle concentration, and pulsating frequency. This correlation is valid for the parameter range and experiment conditions of the current study, and it is not verified for further extrapolation. Figure 9 represents the correlation between the Nu experimental and the Nu predicted.

$$Nu = a * Conc^b + c * frequency^d + e \quad (14)$$

$$friction\ factor = a * Conc^3 + b * Conc^2 + c * Conc^d + e * frequency^f + g \quad (15)$$

where, Conc. = concentration.

The values of constants a, b, c, d, e, f, and g according to the applied case listed are in Table 4.

However, the prediction results by the correlation are correlated to the experimental results, as shown in Figure 9. The correlation coefficient, R2, is positive with a 0.956 value, which indicates the high meaningfulness of the produced correlation, as it is higher than 0.9.

To further demonstrate the ability of the developed correlation to estimate the Nu, Figure 10 has been developed to show the experimental and predicted Nu results. The maximum difference between the experimental and predicted Nu values is 12.4%, and the mean difference over the entire tested CuO-water nanofluid concentration range is 3.96%, which provides further evidence of the correlation accuracy and ability to mathematically predict the Nu for oscillatory CuO-water nanofluid flows.

Table 4. Constant values in Nusselt number and friction factor correlations

Nanofluids	Parameters	Nusselt Number		Friction Factor	
		Continuous flow	Periodic flow	Continuous flow	Periodic flow
With-out Nano	a	0	0	0	0
	b	1	1	0	0
	c	0	0	0	0
	d	1	1	1	1
	e	24.97	25.14	0	0
	f	/	/	1	1
	g	/	/	0.003588	0.006752
	a	0	42322.96	2.025556	1.92
With Nano	b	1	0	-1.721215	-1.63
	c	0	-340.38	98.15	448.34
	d	1	30.25	0.001214	0.00025
	e	24.97	-42281.1	0	64.899
	f	/	/	1	0.00083
	g	/	/	-97.58	-512.74

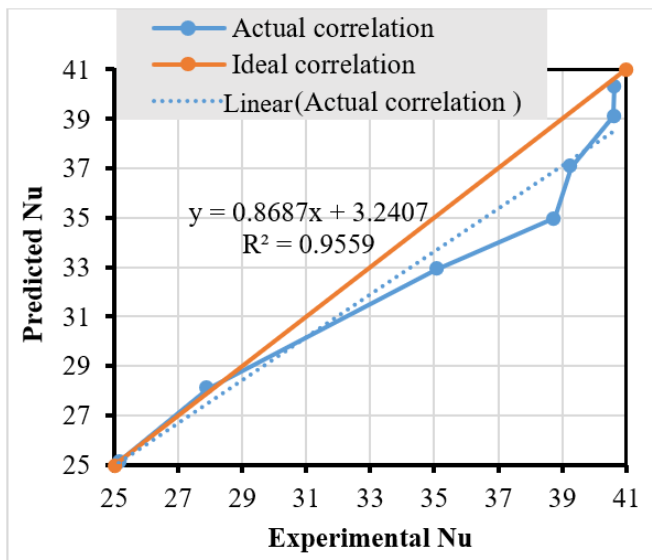


Figure 9. Validation test of the developed correlation for the flow of variable nanoparticle concentrations with 10 Hz oscillation

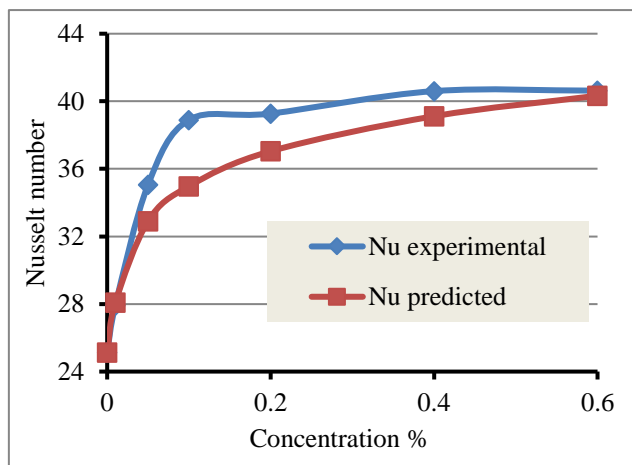


Figure 10. Validation test of the developed correlation for the flow of variable nanoparticle concentrations with 10 Hz oscillation

5. CONCLUSIONS

Both passive and active techniques have a significant

impact on improving heat transfer rates. This research is directed to improve heat transfer without affecting the device design by controlling fluid flow or improving its properties using nanofluids. However, the increase in nanoparticle concentrations leads to problems of sedimentation, high pumping capacity, and higher cost. To eliminate these challenges, the current study investigated the use of low-concentration nanoparticles combined with pulsating flow to enhance the heat transfer rate and minimize the pressure drop. The results reveal that the optimum performance of PHE is achieved at 0.2 wt.% nanoparticle concentration and 10 Hz pulsating frequency. This combination technique enhanced the heat transfer rate while maintaining the pressure drop in the feasible range, representing an effective and cost-saving solution. The nanofluids triggered by pulsating flow can effectively improve the thermal performance of the plate heat exchangers, providing an applicable approach for thermal management in various engineering applications. Further, increasing the number of plates or modifying its height may affect the heat transfer rate and pressure drop parameters, so further investigations in this direction are recommended for future studies. The developed correlation to predict the Nusselt numbers for oscillatory CuO-water nanofluid flow indicated high validity with a 0.95 correlation coefficient.

REFERENCES

- [1] Choi, S.U.S., Eastman, J.A. (1995). Enhancing thermal conductivity of fluids with nanoparticles, developments and applications of non-Newtonian flows. *ASME Journal of Heat Transfer*, 66: 99-105.
- [2] Daungthongsuk, W., Wongwises, S. (2007). A critical review of convective heat transfer of nanofluids. *Renewable and Sustainable Energy Reviews*, 11(5): 797-817. <https://doi.org/10.1016/j.rser.2005.06.005>
- [3] Wang, X.Q., Mujumdar, A.S. (2007). Heat transfer characteristics of nanofluids: A review. *International Journal of Thermal Sciences*, 46(1): 1-19. <https://doi.org/10.1016/j.ijthermalsci.2006.06.010>
- [4] Kakaç, S., Pramuanjaroenkij, A. (2009). Review of convective heat transfer enhancement with nanofluids. *International Journal of Heat and Mass Transfer*, 52(13-14): 3187-3196. <https://doi.org/10.1016/j.ijheatmasstransfer.2009.02.006>
- [5] Godson, L., Raja, B., Mohan Lal, D., Wongwises, S. (2010). Enhancement of heat transfer using nanofluids—

- An overview. *Renewable and Sustainable Energy Reviews*, 14(2): 629-641. <https://doi.org/10.1016/j.rser.2009.10.004>
- [6] Al-Kayiem, H., Lin, S., Lukmon, A. (2013). Review on nanomaterials for thermal energy storage technologies. *Nanoscience & Nanotechnology-Asia*, 3(1): 60-71. <https://doi.org/10.2174/22113525113119990011>
- [7] Sarkar, J. (2011). A critical review on convective heat transfer correlations of nanofluids. *Renewable and Sustainable Energy Reviews*, 15(6): 3271-3277. <https://doi.org/10.1016/j.rser.2011.04.025>
- [8] Al-Kayiem, H.H., Kassim, M.S., Taher, S.T. (2020). Applications of compound nanotechnology and twisted inserts for enhanced heat transfer. *Inverse Heat Conduction and Heat Exchangers*. <https://doi.org/10.5772/intechopen.93359>
- [9] Al-Kayiem, H.H. (2017). Reliability of nanoadditives on the thermal enhancement of nanofluids and nanocomposites. *Nanoscience and Nanotechnology - Asia*, 7(2): 124. <https://doi.org/10.2174/221068120702170801094740>
- [10] Zhang, J., Zhu, X.W., Mondejar, M.E., Haglind, F. (2019). A review of heat transfer enhancement techniques in plate heat exchangers. *Renewable and Sustainable Energy Reviews*, 101: 305–328. <https://doi.org/10.1016/j.rser.2018.11.017>
- [11] Singh, P., Gupta, V.K., Animasaun, I.L., Muhammad, T., Al-Mdallal, Q.M. (2023). Dynamics of Newtonian liquids with distinct concentrations due to time-varying gravitational acceleration and triple diffusive convection: Weakly non-linear stability of heat and mass transfer. *Mathematics*, 11(13): 2907. <https://doi.org/10.3390/math11132907>
- [12] Shamshirgaran, S.R., Al-Kayiem, H.H., Sharma, K.V., Ghasemi, M. (2020). State of the art of techno-economics of nanofluid-laden flat-plate solar collectors for sustainable accomplishment. *Sustainability*, 12(21): 9119. <https://doi.org/10.3390/su12219119>
- [13] Saranya, S., Duraihem, F.Z., Animasaun, I.L., Al-Mdallal, Q.M. (2023). Quartic autocatalysis on horizontal surfaces with an asymmetric concentration: Water-based ternary-hybrid nanofluid carrying titania, copper, and alumina nanoparticles. *Physica Scripta*, 98(7): 075214. <https://doi.org/10.1088/1402-4896/acdb08>
- [14] Wang, F.Z., Al-Mdallal, Q.M., Famakinwa, O.A., Animasaun, I.L., Vaidya, H. (2023). Rayleigh-Benard convection of water conveying copper nanoparticles of larger radius and inter-particle spacing at increasing ratio of momentum to thermal diffusivities. *Alexandria Engineering Journal*, 71: 521–533. <https://doi.org/10.1016/j.aej.2023.03.028>
- [15] Naphon, P., Wiriyaart, S. (2018). Experimental study on laminar pulsating flow and heat transfer of nanofluids in micro-fins tube with magnetic fields. *International Journal of Heat and Mass Transfer*, 118: 297-303. <https://doi.org/10.1016/j.ijheatmasstransfer.2017.10.131>
- [16] Muley, A., Manglik, R.M., Metwally, H.M. (1999). Enhanced heat transfer characteristics of viscous liquid flows in a chevron plate heat exchanger. *Journal of Heat and Mass Transfer*, 121(4): 1011-1017. <https://doi.org/10.1115/1.2826051>
- [17] Khan, T.S., Khan, M.S., Chyu, M.C., Ayub, Z.H. (2010). Experimental investigation of single phase convective heat transfer coefficient in a corrugated plate heat exchanger for multiple plate configurations. *Applied Thermal Engineering*, 30(8-9): 1058-1065. <https://doi.org/10.1016/j.applthermaleng.2010.01.021>
- [18] Kumar, V., Tiwari, A.K., Ghosh, S.K. (2016). Effect of chevron angle on heat transfer performance in plate heat exchanger using ZnO/water nanofluid. *Energy Conversion and Management*, 118: 142-154. <https://doi.org/10.1016/j.enconman.2016.03.086>
- [19] Akhavan-Behabadi, M.A., Shahidi, M., Aligoodarz, M.R. (2015). An experimental study on heat transfer and pressure drop of MWCNT-water nanofluid inside horizontal coiled wire inserted tube. *International Communications in Heat and Mass Transfer*, 63: 62-72. <https://doi.org/10.1016/j.icheatmasstransfer.2015.02.013>
- [20] Xie, H.Q., Yu, W., Li, Y. (2009). Thermal performance enhancement in nanofluids containing diamond nanoparticles. *Journal of Physics D: Applied Physics*, 42(9): 095413. <https://doi.org/10.1088/0022-3727/42/9/095413>
- [21] Jamshidi, N., Farhadi, M., Sedighi, K., Ganji, D.D. (2012). Optimization of design parameters for nanofluids flowing inside helical coils. *International Communications in Heat and Mass Transfer*, 39(2): 311-317. <https://doi.org/10.1016/j.icheatmasstransfer.2011.11.013>
- [22] Corcione, M., Cianfrini, M., Quintino, A. (2012). Heat transfer of nanofluids in turbulent pipe flow. *International Journal of Thermal Sciences*, 56: 58-69. <https://doi.org/10.1016/j.ijthermalsci.2012.01.009>
- [23] Corcione, M., Cianfrini, M., Quintino, A. (2012). Pumping energy saving using nanoparticle suspensions as heat transfer fluids. *Journal of Heat and Mass Transfer*, 134(12): 121701. <https://doi.org/10.1115/1.4007314>
- [24] Corcione, M., Cianfrini, M., Quintino, A. (2013). Optimization of laminar pipe flow using nanoparticle liquid suspensions for cooling applications. *Applied Thermal Engineering*, 50(1): 857-867. <https://doi.org/10.1016/j.applthermaleng.2012.07.029>
- [25] Mukeshkumara, P.C., Kumarb, J., Sureshc, S., Praveen babuc, K. (2012). Experimental study on parallel and counter flow configuration of a shell and helically coiled tube heat exchanger using Al₂O₃ / water nanofluid. *Journal of Materials and Environmental Science*, 3(4): 766-775.
- [26] Kumar, P.C.M., Kumar, J., Sendhilnathan, S., Tamilarasan, R., Suresh, S. (2014). Heat transfer and pressure drop of Al₂O₃ nanofluid as coolant in shell and helically coiled tube heat exchanger. *Bulgarian Chemical Communications*, 46(4): 743.
- [27] Shamshirgaran, S.R., Assadi, M.K., Al-Kayiem, H.H., Sharma, K.V. (2017). Investigation of thermal behaviour, pressure drop, and pumping power in a Cu nanofluid-filled solar flat-plate collector. *MATEC Web of Conferences*, 131: 01003. <https://doi.org/10.1051/mateconf/201713101003>
- [28] Choi, S.U.S., Zhang, Z.G., Yu, W., Lockwood, F.E., Grulke, E.A. (2001). Anomalous thermal conductivity enhancement in nanotube suspensions. *Applied Physics Letters*, 79(14): 2252-2254. <https://doi.org/10.1063/1.1408272>
- [29] Diao, Y.H., Li, C.Z., Zhang, J., Zhao, Y.H., Kang, Y.M.

- (2017). Experimental investigation of MWCNT–water nanofluids flow and convective heat transfer characteristics in multiport minichannels with smooth/micro-fin surface. *Powder Technology*, 305: 206-216. <https://doi.org/10.1016/j.powtec.2016.10.011>
- [30] Oliveira, G.A., Cardenas Contreras, E.M., Bandarra Filho, E.P. (2017). Experimental study on the heat transfer of MWCNT/water nanofluid flowing in a car radiator. *Applied Thermal Engineering*, 111: 1450–1456. <https://doi.org/10.1016/j.applthermaleng.2016.05.086>
- [31] Huang, D., Wu, Z., Sunden, B. (2015). Pressure drop and convective heat transfer of Al_2O_3 /water and MWCNT/water nanofluids in a chevron plate heat exchanger. *International Journal of Heat and Mass Transfer*, 89: 620-626. <https://doi.org/10.1016/j.ijheatmasstransfer.2015.05.082>
- [32] Sarafraz, M.M., Hormozi, F. (2016). Heat transfer, pressure drop and fouling studies of multi-walled carbon nanotube nanofluids inside a plate heat exchanger. *Experimental Thermal and Fluid Science*, 72: 1-11. <https://doi.org/10.1016/j.expthermflusci.2015.11.004>
- [33] Wang, X.F., Zhang, N.L. (2005). Numerical analysis of heat transfer in pulsating turbulent flow in a pipe. *International Journal of Heat and Mass Transfer*, 48(19-20): 3957-3970. <https://doi.org/10.1016/j.ijheatmasstransfer.2005.04.011>
- [34] Alikhan, A.H., Maghrebi, M.J. (2022). Experimental investigation on frequency pulsation effects on a single pass plate heat exchanger performance. *Heat Transfer*, 51(3): 2688-2701. <https://doi.org/10.1002/htj.22420>
- [35] Alasady, A.H., Maghrebi, M.J. (2022). Characterisation of a plate heat exchanger chevron type with carbon-based nanofluids under pulsed condition. *Proceedings of the Institution of Mechanical Engineers, Part C: Journal of Mechanical Engineering Science*, 236(7): 3831-3846. <https://doi.org/10.1177/09544062211042647>
- [36] Najafabadi, M.K., Bognár, G., Hriczó, K. (2022). The effects of water-CuO nanofluid flow on heat transfer inside a heated 2D channel. *Design of Machines and Structures*, 12(1): 47-62. <https://doi.org/10.32972/dms.2022.005>
- [37] Surendar, E., Khadar vali, S., Usha sri, P. (2024). Experimental investigation on enhancement of heat transfer in a straight tube heat exchanger using twisted tape inserts and nano fluids- effect of turbulent and laminar flow characteristics. *MATEC Web Conferences*, 392: 01031. <https://doi.org/10.1051/matecconf/202439201031>
- [38] Kakaç, S., Liu, H. (2002). *Heat Exchangers: Selection, Rating, and Thermal Design*, Second Edition. CRC Press, Boca Raton.
- [39] Das, L., Rubbi, F., Habib, K., Saidur, R., Islam, N., Saha, B.B., Aslfattahi, N., Irshad, K. (2021). Hydrothermal performance improvement of an inserted double pipe heat exchanger with Ionanofluid. *Case Studies in Thermal Engineering*, 28: 101533. <https://doi.org/10.1016/j.csite.2021.101533>

NOMENCLATURE

Cp	specific heat, J/kg·K
f	friction factor
\dot{m}	mass flow rate, kg/s
k	thermal conductivity, W/m·K
Nu	Nusselt number
P	pressure, Pa
PHE	plate heat exchanger
Pr	Prandtl number
Q	heat transfer rate, W
Re	Reynolds number
T	temperature, °C
Δ	difference

Greek symbols

φ	volume fraction
ρ	density, kg/ m ³
μ	viscosity, kg/m·s
ε	effectiveness

Subscripts

avg	average
c	cold
w	water
nf	nanofluid
p	particle
h	hot
i	in
o	out
r	relative